Iron Porphyrin Dications with Neutral Axial Ligands: DFT Calculations Delineate Similarities with Heme Protein Compound II Intermediates

ARTICLE *in* THE JOURNAL OF PHYSICAL CHEMISTRY B · MARCH 2011

Impact Factor: 3.3 · DOI: 10.1021/jp111109e · Source: PubMed

4 AUTHORS, INCLUDING:

Mikio Nakamura
Toho University
177 PUBLICATIONS **2,659** CITATIONS
SEE PROFILE

Abhik Ghosh
UiT - The Arctic University of Norway
187 PUBLICATIONS **5,401** CITATIONS
SEE PROFILE

THE JOURNAL OF PHYSICAL CHEMISTRY B

ARTICLE

pubs.acs.org/JPCB

Iron Porphyrin Dications with Neutral Axial Ligands: DFT Calculations Delineate Similarities with Heme Protein Compound II Intermediates

Adam C. Chamberlin,[†] Akira Ikezaki,[‡] Mikio Nakamura,[*,‡,§] and Abhik Ghosh[*,†]

[†]Department of Chemistry and Center for Theoretical and Computational Chemistry, University of Tromsø, 9037 Tromsø, Norway

[‡]Department of Chemistry, School of Medicine, Toho University, Ota-ku, Tokyo, 143-8540, Japan

[§]Division of Chemistry, Graduate School of Science, Toho University, Funabashi, 274-8510, Japan

Supporting Information

ABSTRACT: OLYP/TZP calculations on two symmetrized model complexes $[Fe(TPP)(py)_2]^{2+}$ and $[Fe(TPP)(PhNC)_2]^{2+}$ (TPP = *meso*-tetraphenylporphyrin, py = pyridine, PhNC = phenylisocyanide) reveal dense manifolds of low-energy electronic states. For the latter complex, broken-symmetry calculations successfully reproduce the unique $S = 0$ ground state that is expected on the basis of experimental measurements on a closely related complex; the $S = 0$ state arises from antiferromagnetic coupling between a low-spin $d_{xy}^1(d_{xz},d_{yz})^4$ Fe(III) center and a porphyrin "a_{2u}" radical. Furthermore, the calculations indicate low-energy Fe(IV) states for both complexes. Overall, the results contribute to our deepening understanding of the factors contributing to the stability of iron(IV) centers. Thus, a dianionic π-donor oxo ligand is no longer deemed a requirement for the stability of heme-based Fe(IV) centers; iron(IV) intermediates of heme proteins such as chloroperoxidase, catalase, and MauG, having only monanionic ligands such as hydroxide, thiolate, and phenolate and/or (in the case of MauG) a neutral histidine as axial ligands, are now firmly established.

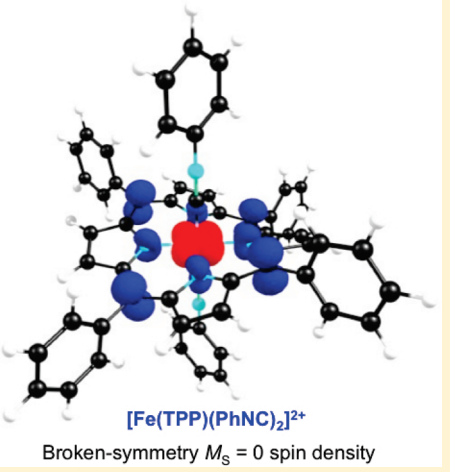

INTRODUCTION

Iron(IV)-oxo and -hydroxo intermediates are the key reactive species of a number of heme and nonheme iron enzymes.[1−3] For a number of these species, particularly the so-called compound II intermediates, a fundamental theoretical question concerns how a highly oxidizing iron(IV) center coexists in contact with an easily oxidized porphyrin ligand.[4,5] Anionic axial ligands such as alkoxide,[6] thiolate,[7−9] and phenolate[10,11] undoubtedly play a role,[12] as does ligand noninnocence,[5,13,14] at least in certain cases. Also intriguing in this connection are synthetic model heme dications with neutral axial ligands such as N-heteroaromatic bases[15,16] and isocyanides.[17] Like enzymatic compound II intermediates, these species are two oxidation equivalents above Fe(II); their electronic structures, however, remain less explored. A variety of electronic configurations may be envisioned for them, including low-spin Fe(IV) configurations and various low-spin Fe(III) porphyrin radicals. A priori, we might conjecture that a number of these states would be roughly equienergetic; for other states, we are unable to advance even an "educated guess" about their relative energies. In this study, we have explored the possibility that density functional theory (DFT) calculations might provide a reasonable picture of this, supposedly, very rich spin state manifold.

From the outset, we believed that there was a fair chance that DFT should afford a reasonable description of the most relevant dication states. Common DFT methods often perform poorly in describing the relative energetics of states with widely different spin multiplicities such as high- and low-spin iron(III) states.[18,19] In this problem, however, the iron center, whether it is Fe(III) or Fe(IV), is low-spin throughout, and we are exclusively concerned with spin-zero and spin-one states.[20,21] With the OLYP functional,[22,23] which has often proved superior to other functionals in calculations of transition metal spin state energetics,[24−26] and careful use of group theory, we chose to calculate a number of electronic states of two symmetrized model complexes, $[Fe(TPP)(py)_2]^{2+}$ and $[Fe(TPP)(PhNC)_2]^{2+}$, where py = pyridine and PhNC = phenylisocyanide. These two complexes may be viewed as idealized models of the less symmetric complexes $[Fe(Por)(HIm)_2]^{2+}$ (where Por = an arbitrary porphyrin and ImH = imidazole)[15,17] and $[Fe(Por)(^tBuNC)_2]^{2+}$,[17] respectively. The choice of these two types of complexes was deliberate and is related to their different ground state spin multiplicities. Thus, whereas the bis(imidazole) and presumably the bis(pyridine) complexes are paramagnetic ($S = 1$), the bis(isocyanide) complex is diamagnetic ($S = 0$); these different

Received: November 21, 2010
Revised: February 20, 2011

Table 1. OLYP/TZP Results on Low-Energy States of $[Fe(TPP)(py)_2]^{2+}$:[a] Electronic Configurations, All-Electron Occupations ($\alpha||\beta$), and Relative Energies (eV)

state	Fe config.	TPP config.	$Fe^{III}-TPP^{\bullet-}$ coupling	S	occupations: $\alpha\|\beta$	E (eV)	$<S^2>$
A	Fe(III): $d_{xz}^2 d_{yz}^1 d_{xy}^2$	a_{2u}^1	ferro.	1	A 57 // 57 B1 54 // 53 B2 52 // 52 B3 52 // 51	0.00	2.022
B	Fe(III): $d_{xz}^2 d_{yz}^2 d_{xy}^1$	a_{2u}^1	antiferro. (broken-symmetry)	0	A 57 // 57 B1 53 // 53 B2 52 // 52 B3 52 // 52	0.12	0.548
C	Fe(III): $d_{xz}^2 d_{yz}^2 d_{xy}^1$	a_{2u}^1	ferro.	1	A 57 // 57 B1 54 // 52 B2 52 // 52 B3 52 // 52	0.28	2.027
D	Fe(IV): $d_{xz}^1 d_{yz}^1 d_{xy}^2$	TPP^{2-}	n.a.	1	A 57 // 57 B1 54 // 54 B2 52 // 51 B3 52 // 51	0.30	2.035
E	Fe(III): $d_{xz}^1 d_{yz}^2 d_{xy}^2$	a_{1u}^1	ferro.	1	A 57 // 56 B1 54 // 54 B2 52 // 51 B3 52 // 52	0.41	2.020
F	Fe(III): $d_{xz}^2 d_{yz}^2 d_{xy}^1$	a_{1u}^1	antiferro.	0	A 56 // 57 B1 54 // 53 B2 52 // 52 B3 52 // 52	0.42	1.038
G	Fe(III): $d_{xz}^2 d_{yz}^2 d_{xy}^1$	a_{1u}^1	ferro.	1	A 57 // 56 B1 54 // 53 B2 52 // 52 B3 52 // 52	0.44	2.011
H	Fe(IV): $d_{xz}^2 d_{yz}^1 d_{xy}^1$	Saddled TPP^{2-} (C_{2v})	n.a.	1	A1 73 // 72 A2 38 // 38 B1 52 // 52 B2 52 // 51	0.71	3.094

[a] All calculations were carried out with D_2 symmetry, except for **H**, which was optimized under C_{2v}.

Table 2. Mulliken Spin Populations for Low-Energy States of $[Fe(TPP)(py)_2]^{2+}$[a]

	A	B	C	D	E	F	G	H
Fe	1.0868	0.7720	1.1322	1.5158	0.9700	0.8004	0.7914	0.9700
N_1	0.0512	−0.0431	0.0442	0.0430	−0.0269	0.0663	−0.0008	−0.0490
N_2	0.0833	−0.0378	0.0435	0.0431	−0.0490	0.0668	−0.0003	−0.0269
C_α	−0.0234	0.0117	−0.0277	−0.0006	0.1311	−0.1529	0.1154	0.1369
C_β	−0.0029	−0.0062	0.0028	0.0585	0.0475	−0.0229	0.0126	0.0153
C_{meso}	0.1513	−0.1100	0.1745	−0.0077	−0.0527	0.1243	0.0230	−0.0527
$C_{ipso,Ph}$	−0.0026	−0.0012	0.0032	0.0009	0.0005	−0.0048	−0.0044	0.0006
$C_{o,Ph}$	0.0137	−0.0126	0.0182	−0.0002	0.0099	−0.0045	0.0105	0.0100
$C_{m,Ph}$	−0.0034	0.0037	−0.0050	0.0003	0.0134	−0.0145	0.0154	0.0132
$C_{p,Ph}$	0.0219	−0.0231	0.0331	−0.0002	−0.0054	0.0058	−0.0053	−0.0054
$N_{pyridine}$	−0.0229	−0.0168	−0.0212	−0.0431	−0.0264	−0.0114	−0.0115	−0.0264
$C_{\alpha,pyridine}$	0.0018	−0.0032	−0.0026	0.0032	0.0026	−0.0029	−0.0033	0.0027

[a] N_1 and N_2 refer to opposite pairs of porphyrin nitrogens; the N_2-N_2 axis is shorter than the N_1-N_1 axis.

ground states provide valuable calibration of the overall body of our computational results. We were pleased to find that our calculations provide a credible and remarkably complete description of the electronic state manifolds of iron porphyrin dications.

METHODS

All calculations were carried out with the OLYP[22,23] exchange-correlation functionals, STO-TZP basis sets, a suitably fine grid for numerical integration of matrix elements, and tight convergence criteria for both SCF and geometry iterations, all as implemented in the ADF 2007 program system.[27] We made full use of point group symmetry to calculate the different electronic configurations of interest. The maximum possible symmetry for the ruffled conformations of both $[Fe(TPP)(py)_2]^{2+}$ and $[Fe(TPP)(PhNC)_2]^{2+}$ is D_{2d}. Certain states, however, are degenerate (^2E) under D_{2d} so, to allow for Jahn−Teller distortions, the great majority of the calculations were carried out simply with D_2 (or C_{2v}), which does not have degenerate representations.

RESULTS

(a). Monocations. Monocationic iron(III) porphyrins with bis(pyridine) and bis(isocyanide) axial ligation have been extensively

dx.doi.org/10.1021/jp111109e |J. Phys. Chem. B XXXX, XXX, 000–000

Table 3. OLYP/TZP Results on Low-Energy States of $[Fe(TPP)(PhNC)_2]^{2+}$:[a] Electronic Configurations, All-Electron Occupations ($\alpha||\beta$), and Relative Energies (eV)

state	Fe config.	TPP config.	$Fe^{III}-TPP^{\bullet-}$ coupling	S	occupations: $\alpha\|\|\beta$	E (eV)	$<S^2>$
P	Fe(III): $d_{xz}^2 d_{yz}^2 d_{xy}^1$	a_{2u}^1	antiferro. (broken-symmetry)	0	A1 47 // 47	0.00	0.406
					A2 12 // 12		
					B1 14 // 14		
					B2 45 // 45		
					E 108 // 108		
Q	$d_{xz}^1 d_{yz}^2 d_{xy}^2$	a_{2u}^1	ferro.	1	A1 93 // 92	0.03	2.022
					A2 26 // 26		
					B1 54 // 54		
					B2 54 // 53		
R	Fe(III): $d_{xz}^2 d_{yz}^2 d_{xy}^1$	a_{1u}^1	antiferro.	0	A1 47 // 47	0.13	1.033
					A2 12 // 12		
					B1 13 // 14		
					B2 46 // 45		
					E 108 // 108		
S	Fe(III): $d_{xz}^2 d_{yz}^2 d_{xy}^1$	a_{1u}^1	ferro.	1	A1 47 // 47	0.16	2.005
					A2 12 // 12		
					B1 14 // 13		
					B2 46 // 45		
					E 108 // 108		
T	Fe(III): $d_{xz}^2 d_{yz}^2 d_{xy}^1$	a_{2u}^1	ferro.	1	A1 47 // 47	0.19	2.033
					A2 12 // 12		
					B1 14 // 14		
					B2 46 // 44		
					E 108 // 108		
U	Fe(IV): $d_{xz}^1 d_{yz}^1 d_{xy}^2$	TPP^{2-}	n.a.	1	A1 47 // 47	0.45	2.023
					A2 12 // 12		
					B1 14 // 14		
					B2 46 // 46		
					E 108 // 106		

[a] Except for **Q**, which was optimized under C_{2v}, all states were optimized with D_2 symmetry constraints.

Table 4. Mulliken Spin Populations for Low-Energy States of $[Fe(TPP)(PhNC)_2]^{2+}$

	P	Q	R	S	T	U
Fe	0.6315	0.8532	0.5252	0.5201	1.1235	1.2257
N	−0.0474	0.1148	0.0995	0.0307	0.0717	0.0718
C_α	0.0189	−0.0471	−0.1623	0.1087	−0.0404	−0.0035
$C_{\alpha'}$	-	−0.0252	-	-	-	-
C_β	−0.0041	0.0438	−0.0233	0.0125	0.0046	0.0709
$C_{\beta'}$	-	0.0038	-	-	-	-
C_{meso}	−0.1269	0.2007	0.1718	0.0710	0.2327	−0.0076
$C_{meso'}$	-	0.1903	-	-	-	-
$C_{isocyanide}$	0.0184	−0.0117	−0.0029	−0.0039	−0.0432	−0.0223
$C_{isocyanide'}$	-	−0.0314	-	-	-	-
$N_{isocyanide}$	0.0083	0.0068	−0.0056	−0.0050	0.0130	−0.0016
$N_{isocyanide'}$	-	0.0149	-	-	-	-

studied as models of biological ferriheme sites such as those in the cytochromes *b*.[28] The overall conclusion from NMR and EPR spectroscopy is that whereas six-coordinate iron(III) porphyrins generally favor a $d_{xy}^2(d_{xz},d_{yz})^3$ ground state (henceforth referred to simply as d_π^1) low-basicity pyridines such as 4-cyanopyridine and even stronger π-acceptors such as isocyanides result in an unusual $d_{xy}^1(d_{xz},d_{yz})^4$ state (henceforth referred to as d_δ^1), as a result of strong stabilization of the d_π^1 orbitals.[29,30] Because these monocationic species have already been the subject of an earlier DFT study,[31] here we will only address them briefly. Their main relevance to this study is that they provide a useful calibration of the OLYP/TZP method.

We have found that OLYP/TZP calculations predict essentially isoenergetic d_π^1 and d_δ^1 states for $[Fe(TPP)(py)_2]^+$; the minimum-energy conformations of both states correspond to a pair of orthogonal pyridine ligands with the pyridine planes containing a pair of opposite *meso* carbons. It thus appears that our calculations slightly overstabilize the d_δ^1 state relative to the d_π^1 state. For $[Fe(TPP)(PhNC)_2]^+$, our calculations yield the expected d_δ^1 ground state; the d_π^1 state was found to be 0.29 eV higher in energy, and the low-spin iron(II) porphyrin a_{1u}-radical state was found to be 0.51 eV above the ground state. These spin state energetics data for the monocations should allow for a more informed appreciation of the energetics of the dication electronic states.

(b). $[Fe(TPP)(py)_2]^{2+}$. Table 1 presents key low-energy states, including qualitative descriptions, all-electron occupations, and OLYP/TZP relative energies, for $[Fe(TPP)(py)_2]^{2+}$. As in the

dx.doi.org/10.1021/jp111109e |*J. Phys. Chem. B* XXXX, XXX, 000–000

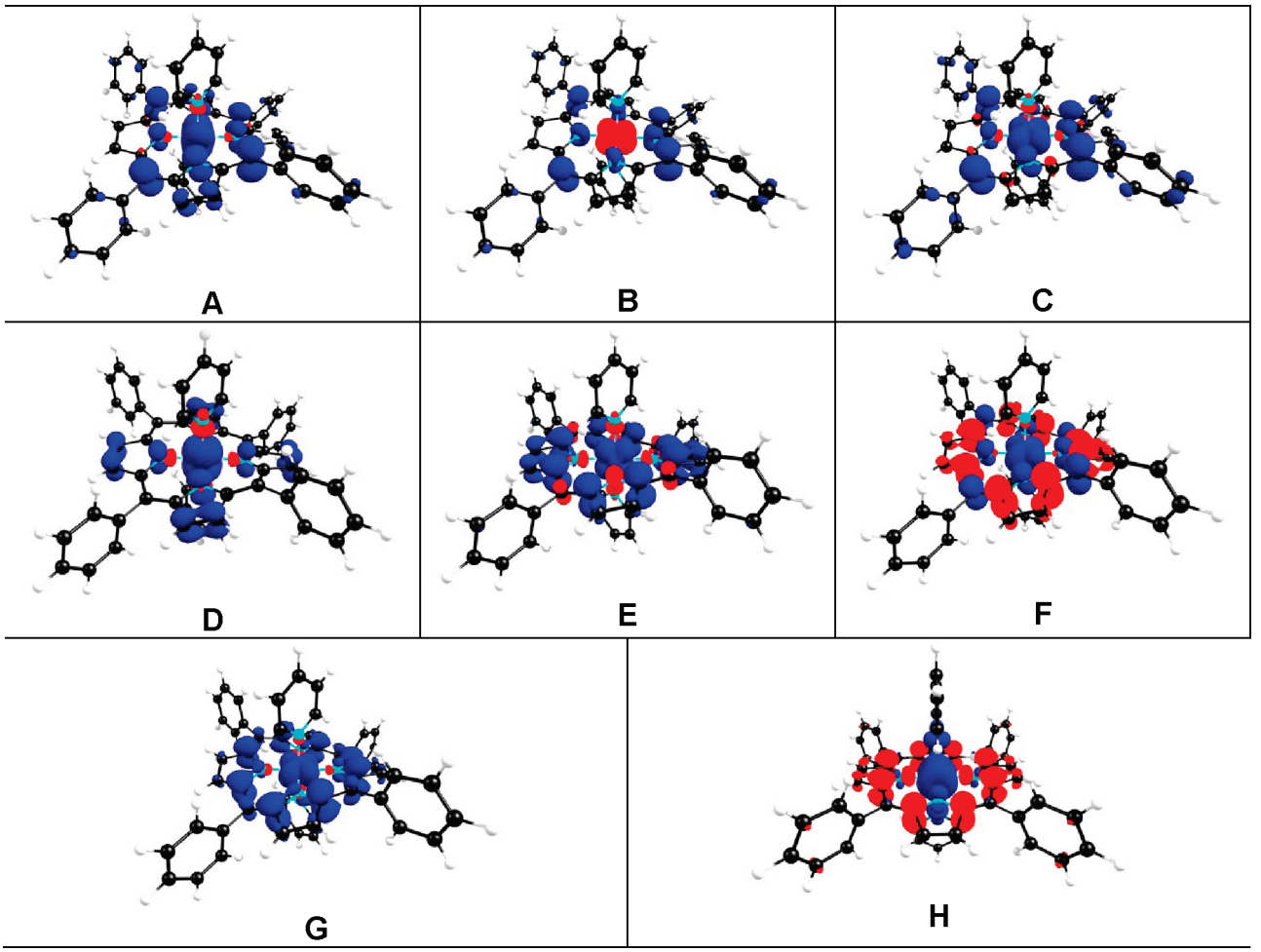

Figure 1. OLYP/TZP spin densities for different low-energy states of $[Fe(TPP)(py)_2]^{2+}$.

case of the corresponding monocation, the low-energy states all have a pair of orthogonal pyridine ligands with the pyridine planes containing a pair of opposite *meso* carbons. Such an axial ligand conformation is consistent with ruffling of the porphyrin macrocycle. Regardless of the electronic state, the alternate conformation, where the pyridine planes are aligned along the $Fe-N_{Por}$ vectors, was found to be rather high in energy (at least 0.7 eV above the ground state), and these states will not be described any further. As shown in Table 1, making judicious use of group theory, we found as many as seven electronic states (A−G) within 0.5 eV of the lowest-energy state. Figure 1 presents spin density plots for these states and Table 2 selected symmetry-distinct spin populations. Although we will not comment much on the spin densities, the reader may find it useful to verify that they indeed are consistent with the stated orbital occupancies.

The ground state (**A** in Table 1), in this OLYP/TZP study, corresponds to a $d_{xy}^2(d_{xz},d_{yz})^3$ Fe(III) porphyrin a_{2u} radical; however, because the d_{xy} and the porphyrin a_{2u} orbitals both transform as b_1 under D_2 and indeed overlap in the ruffled conformation, the electronic structure is also describable as Fe(IV) with a $d_{xy}^1(d_{xz},d_{yz})^3$ conformation. The $d_{xy}-a_{2u}$ overlap leads to a distinctly ruffled conformation for this state. As shown in Figure 1, majority spin density in this state is found both on the *meso* carbons and on a pair of antipodal $C_\beta-C_\beta$ bonds.

Slightly higher in energy are a pair of $d_{xy}^1(d_{xz},d_{yz})^4$ Fe(III) porphyrin a_{2u} radical states (**B** and **C**); the two states are 0.12 and 0.28 eV above the lowest-energy state and feature metal−porphyrin antiferromagnetic and ferromagnetic coupling, respectively. Although the relative stability of a_{2u} radical states is expected for TPP derivatives, we have noted above that these calculations may somewhat overstabilize a d_δ^1 Fe(III) center relative to a d_π^1 one. The real energies of these two states thus may be slightly higher than those found here.

Next in energy at 0.3 eV is a so-called $S = 1$ Fe(IV) state (**D**) with $d_{xy}^2(d_{xz},d_{yz})^2$ configuration; note from Figure 1 the cylindrical spin density on the iron and also the fact that a considerable amount of spin density delocalizes onto the porphyrin as a result of interactions involving the Fe d_π orbitals and the porphyrin e_g HOMOs.[32]

At 0.40−0.45 eV above the ground state are the Fe(III) porphyrin a_{1u} radical states (**E**−**G**); the iron center in these states is either $d_{xy}^2(d_{xz},d_{yz})^3$ or $d_{xy}^1(d_{xz},d_{yz})^4$. Given the orthogonality of the magnetic orbitals, it is not particularly surprising that the ferromagnetic versus antiferromagnetic nature of the metal−porphyrin spin coupling does not affect the energies of these states very much.

(c). $[Fe(TPP)(PhNC)_2]^{2+}$. Table 3 lists key low-energy states calculated for $[Fe(TPP)(PhNC)_2]^{2+}$, and Table 4 presents selected symmetry-distinct spin populations. Figure 2 presents

dx.doi.org/10.1021/jp111109e |*J. Phys. Chem. B* XXXX, XXX, 000–000

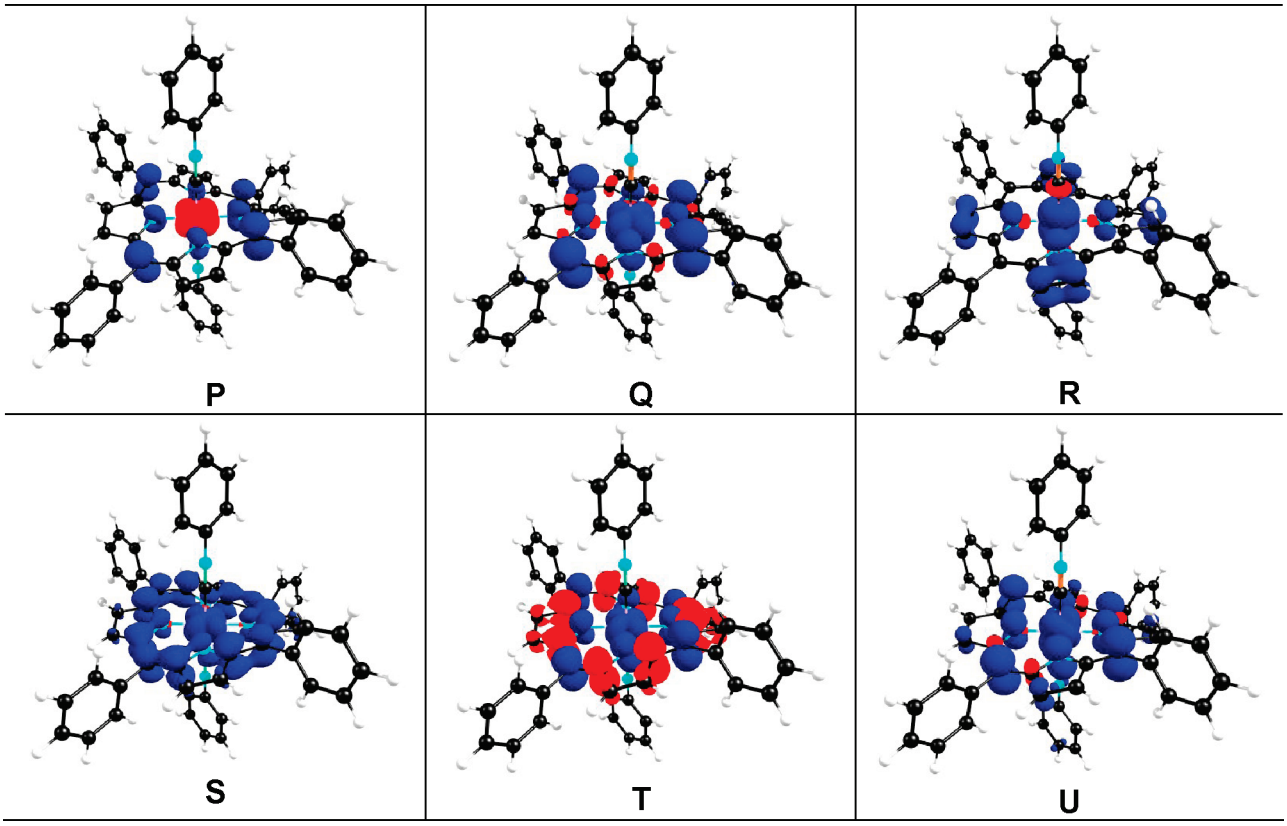

Figure 2. OLYP/TZP spin densities for different low-energy states of $[Fe(TPP)(PhNC)_2]^{2+}$.

the spin density plots for these states. Consistent with experimental results on $[Fe(TMP)(^tBuNC)_2]^{2+}$,[17] our calculations reproduce a singlet state as the lowest-energy state for $[Fe(TPP)(PhNC)_2]^{2+}$. This state (denoted **P** in Table 3) has a $d_{xy}^1(d_{xz},d_{yz})^4$ Fe(III) center antiferromagnetically coupled to a porphyrin a_{2u} radical. This description is supported by the broken-symmetry spin density plot (Figure 2) and the corresponding spin populations (Table 4). (It may be recalled that the $M_S = 0$ broken-symmetry state is not the true $S = 0$ ground state, even though it may be viewed as a fair approximation; the spin populations for this occupation thus are not real.) The corresponding ferromagnetically coupled, $S = 1$ state (**T**) is found to be 0.19 eV higher in energy. Our calculations also indicate rather low energies for $d_{xy}^1(d_{xz},d_{yz})^4$ Fe(III) a_{1u} radical states: 0.13 eV for metal−porphyrin antiferromagnetic coupling (**R**) and 0.16 eV for ferromagnetic coupling (**S**).

Considering the strongly π-accepting nature of the isocyanide ligands, electronic states with unpaired d_π electrons might have been expected to be quite high in energy. Yet the $d_{xy}^2(d_{xz},d_{yz})^2$ Fe(IV) state (**U**) is found to be only 0.45 eV above the ground state. Somewhat curiously, the $d_{xy}^2(d_{xz},d_{yz})^3$ Fe(III) a_{2u} radical state (**Q**), which may also be viewed as a $d_{xy}^1(d_{xz},d_{yz})^3$ Fe(IV) state (because the d_{xy} and a_{2u} orbitals belong to the same irrep and overlap), is found to be only 0.03 eV above the ground state. Considering that ^{1}H NMR spectroscopy does not reveal a paramagnetic state for $[Fe(TMP)(^tBuNC)_2]^{2+}$,[17] the exceedingly low energy of this state is probably somewhat unphysical and hence a reflection of the imperfect quality of our calculations. Yet the error in the energy is not expected to be large: qualitatively, the degree of ligand noninnocence of this state is no different from that found for a number of other states, for which our calculations have yielded intuitively reasonable results.

CONCLUDING REMARKS

The above calculations clearly extend our understanding of the factors influencing the stability of iron(IV) centers in heme derivatives. Although the two dicationic complexes studied in this work are low-spin Fe(III) porphyrin radicals, the calculations indicate low-energy iron(IV) states no more than a few tenths of an electronvolt above the ground states. These findings resonate well with the recent literature on biological and biomimetic iron(IV) intermediates. Thus, many compound II intermediates are now recognized as iron(IV)-hydroxo species, as opposed to iron(IV)-oxo.[6−12] Similarly, a fair number of iron(IV)-oxo intermediates, unsupported by dianionic porphyrin ligands, have recently been characterized for nonheme systems, both enzymatic[33] and synthetic.[34,35] The old paradigm where iron(IV) was only thought to be stabilized by a dianionic oxo ligand, in conjunction with a dianionic porphyrin, has thus clearly shifted. A particularly instructive case in point is a diiron(IV) intermediate of MauG, a diheme enzyme with two *c*-type hemes, which catalyzes a six-electron oxidation in the biosynthesis of the tryptophan tryptophylquinone cofactor of methylamine dehydrogenase.[36] One of these two iron(IV) centers has been suggested to be a unique, monocationic $[Fe^{IV}(Por)(His)(O\text{-}Tyr)]^+$ site.[37,38]

A second and related lesson from this study, as well as from other studies from our laboratory[39] and elsewhere,[3] concerns the quasi-degenerate nature of many high-valent complexes. Thus, the unique, unambiguous ground states observed are often a façade, giving little indication of a dense manifold of additional states a mere couple of tenths of an electronvolt higher in energy. Temperature-dependent NMR (and EPR) studies are thus essential for experimental studies for such systems, even though these

dx.doi.org/10.1021/jp111109e |*J. Phys. Chem. B* XXXX, XXX, 000–000

measurements too fail to reveal states with energies that are just above what is thermally attainable. Yet such low-energy states are a key part of the overall electronic character of the complexes in question, and it is important to be mindful of their existence when considering their reactivity.

■ ASSOCIATED CONTENT

Supporting Information. Optimized Cartesian coordinates for the various complexes studied in this work. This material is available free of charge via the Internet at http://pubs.acs.org.

■ ACKNOWLEDGMENT

This work was supported by the Research Council of Norway and by a Grant-in-Aid for Scintific Research from the Ministry of Education, Culture, Sports, Science and Technology, Japan.

■ REFERENCES

(1) Ortiz de Montellano, P. R. *Chem. Rev.* **2010**, *110*, 932–948.
(2) Groves, J. T. *J. Inorg. Biochem.* **2006**, *100*, 434–447.
(3) Shaik, S.; Cohen, S.; Wang, Y.; Chen, H.; Kumar, D.; Thiel, W. *Chem. Rev.* **2010**, *110*, 949–1017.
(4) Conradie, J.; Wasbotten, I.; Ghosh, A. *J. Inorg. Biochem.* **2006**, *100*, 502–506.
(5) For the possibility of a noninnocent porphyrin in a minor species of chloroperoxidase compound II, see: Lai, W.; Chen, H.; Shaik, S. *J. Phys. Chem. B* **2009**, *113*, 7912–7917.
(6) Groves, J. T.; Quinn, R.; McMurry, T. J.; Nakamura, M.; Lang, G.; Boso, B. *J. Am. Chem. Soc.* **1985**, *107*, 354–360.
(7) Green, M. T.; Dawson, J. H.; Gray, H. B. *Science* **2004**, *304*, 1653–1656.
(8) Stone, K. L.; Hoffart, L. M.; Behan, R. K.; Krebs, C.; Green, M. T. *J. Am. Chem. Soc.* **2006**, *128*, 6147–6153.
(9) Behan, R. K.; Hoffart, L. M.; Stone, K. L.; Krebs, C.; Green, M. T. *J. Am. Chem. Soc.* **2006**, *128*, 11471–11474.
(10) Horner, O.; Oddou, J. L.; Mouesca, J. M.; Jouve, H. M. *J. Inorg. Biochem.* **2006**, *100*, 477–479.
(11) Rovira, C. *ChemPhysChem* **2005**, *6*, 1820–1826.
(12) Hersleth, H. P.; Ryde, U.; Rydberg, P.; Görbitz, C. H.; Andersson, K. K. *J. Inorg. Biochem.* **2006**, *100*, 460–476.
(13) The compound I intermediates provide the best known examples of noninnocent porphyrin ligands in biology. For a review of the classic literature, see: Terner, J.; Palaniappan, V.; Gold, A.; Weiss, R.; Fitzgerald, M. M.; Sullivan, A. M.; Hosten, C. M. *J. Inorg. Biochem.* **2006**, *100*, 480–501.
(14) The long sought-after Compound I of cytochrome P450 has just been reported: Rittle, J.; Green, M. T. *Science* **2010**, *330*, 933–937.
(15) Goff, H. M.; Philippi, M. A. *J. Am. Chem. Soc.* **1983**, *105*, 7567–7571.
(16) Nakamura, M.; Kawasaki, Y. *Chem. Lett.* **1996**, *25*, 85–86.
(17) Ikezaki, A.; Tukada, H.; Nakamura, M. *Chem. Commun.* **2008**, 2257–2259.
(18) Ghosh, A.; Taylor, P. R. *Curr. Opin. Chem. Biol.* **2003**, *7*, 113–124.
(19) Ghosh, A. *J. Biol. Inorg. Chem.* **2006**, 712–724.
(20) DFT calculations provide an excellent description of metal- versus ligand-centered reduction in nickel hydroporphyrins: Ryeng, H.; Gonzalez, E.; Ghosh, A. *J. Phys. Chem. B* **2008**, *112*, 15158–15173.
(21) DFT calculations appear to provide a good description of singlet−triplet splittings of ruthenium(IV) porphyrins: Gonzalez, E.; Brothers, P. J.; Ghosh, A. *J. Phys. Chem. B* **2010**, *114*, 15380–15388.
(22) The OPTX exchange functional: Handy, N. C.; Cohen, A. *J. Mol. Phys.* **2001**, *99*, 403–412.
(23) The LYP correlation functional: Lee, C.; Yang, W.; Parr, R. G. *Phys. Rev.* **1988**, *B37*, 785–789.
(24) Conradie, J.; Ghosh, A. *J. Chem. Theory Comput.* **2007**, *3*, 689–702.
(25) Swart, M. *J. Chem. Theory Comput.* **2008**, *4*, 2057–2066.
(26) Conradie, M. M.; Conradie, J.; Ghosh, A. *J. Inorg. Biochem.* **2011**, *105*, 84–91.
(27) For a description of the methods used in ADF, see: Velde, G. T.; Bickelhaupt, F. M.; Baerends, E. J.; Guerra, C. F.; Van Gisbergen, S. J. A.; Snijders, J. G.; Ziegler, T. *J. Comput. Chem.* **2001**, *22*, 931–967.
(28) Walker, F. A. In *The Porphyrin Handbook*; Kadish, K. M., Smith, K. M., Guilard, R., Eds.; Academic: San Diego, CA, 2000; Vol. 5, Chapter 36, pp 81−183.
(29) Simmoneaux, G.; Hindre, F.; Le Plouzennec, M. *Inorg. Chem.* **1989**, *28*, 823–825.
(30) Walker, F. A.; Nasri, H.; Turowska-Tyrk, I.; Mohanrao, K.; Watson, C. T.; Shokhirev, N. V.; Debrunner, P. G.; Scheidt, W. R. *J. Am. Chem. Soc.* **1996**, *118*, 12109–12118.
(31) Ghosh, A.; Gonzalez, E.; Vangberg, T. *J. Phys. Chem. B* **1999**, *103*, 1363–1367.
(32) In an earlier PW91 study of this dication, we found this state to be among the lowest in energy. A plausible explanation is that the classic pure functional PW91 favors a high-valent Fe(IV) state, relative to OLYP, which may favor a more noninnocent description: Conradie, J.; Ghosh, A. *J. Phys. Chem. B* **2003**, *107*, 6486–6490.
(33) Krebs, C.; Fujimori, D. G.; Walsh, C. T.; Bollinger, J. M. *Acc. Chem. Res.* **2007**, *40*, 484–492.
(34) Que, L., Jr. *Acc. Chem. Res.* **2007**, *40*, 493–500.
(35) Nam, W. *Acc. Chem. Res.* **2007**, *40*, 522–531.
(36) For a review, see: Wilmot, C. M.; Davidson, V. L. *Curr. Opin. Chem. Biol.* **2009**, *13*, 469–474.
(37) Li, X.; Fu, R.; Lee, S.; Krebs, C.; Davidson, V. L.; Liu, A. *Proc. Natl. Acad. Sci. U.S.A.* **2008**, *105*, 8597–8600.
(38) Ling, Y.; Davidson, V. L.; Zhang, Y. *J. Phys. Chem. Lett.* **2010**, *1*, 2936–2939.
(39) For a study of the low-energy spin states of FeCl corrole, see: Roos, B. O.; Veryazov, V.; Conradie, J.; Taylor, P. R.; Ghosh, A. *J. Phys. Chem. B* **2008**, *112*, 14099–14102.